

H₂O and fat imaging

Xu Feng

Outline

- Introduction
benefit from the separation of water and fat imaging
- Chemical Shift
definition of chemical shift
origin of chemical shift
equations of chemical shift
- Chemical Shift Misregistration Artifacts (CSMA)
definition of CSMA
frequency encoding
slice selection
phase encoding
- H₂O/fat Signal Separation Methods
frequency-selective pulse
tissue nulling with inversion recovery
Dixon method: theory and disadvantage

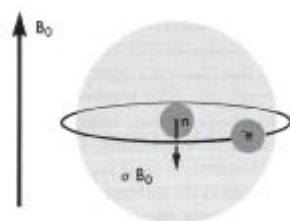
Introduction

- There many parts of the body will **benefit** from good water/fat separation
Like: optic nerve, bone marrow, breast, heart and knee
- Separating water and fat leads to two separate images with **improved contrast and a reduction of artifacts** caused by the interference of fat and water
- **Quantification** of how much fat or water (i.e., their relative **spin densities**) is in a given voxel for a given tissue can also be of clinical value

Chemical Shift

- The frequency at which transverse magnetization precesses **depends slightly on the molecular environment**
- The precessional frequency for magnetization from a watery tissue, such as muscle, is about 3.5 parts per million (ppm) greater than that for adipose tissue
- This spread of precessional frequencies is called **the chemical shift**
- The chemical shift expressed in ppm is **independent of magnetic field**

Origin of Chemical Shift



$$B = B_0 - \sigma B_0 = B_0 (1 - \sigma)$$

Figure 16-1. Origin of the chemical shift. Electrons (e^-) of an atom precess around the direction of the external magnetic field B_0 . This spinning motion of electrons produces an additional local magnetic field, σB_0 , experienced by the nucleus (n), with the shielding constant σ specific to the molecular structure. The effective field B experienced by the nucleus differs from that of the external field B_0 by the amount σB_0 . The resulting alteration of the resonance frequency, γB , called the chemical shift, provides a mechanism for separating the contributions of chemically different nuclei to the MR spectrum.

Chemical Shift

- Larmor Frequency equation:

$$u_0 = gB_0$$

- The resulting local field B (B_{loc}) is proportional to the strength of the external field

$$B_{loc} = \sigma B_0$$

where σ is the dimensionless shielding constant

- The local resonance frequency is given:

$$u = gB_0 - gB_{loc} = gB_0 - g\sigma B_0 = g(1 - \sigma)B_0$$

- The **actual chemical shift** ($du = -g\sigma B_0 = -\sigma u_0$) is proportional to the applied magnetic field

Problems with Fat and Water Signals

- In conventional 2D spin-echo MRI, an image is created through the selection of a slice, the spatial encoding of signals from this slice in the phase and frequency direction, followed by the Fourier transform of the raw data. In each of these steps, fat magnetization, by virtue of chemical shift, will have a different behavior than the magnetization of water

Chemical Shift Misregistration Artifacts (CSMAs)

- The frequency (chemical) shift between water and fat resonance can appear in an image as a spatial mismatching of the two components

If tuned to the frequency of water, fat will be spatially misrepresented. Conversely, tuned to fat, water will be misrepresented.
- These spatial misrepresentations is called **chemical shift misregistration artifacts (CSMAs)**

Which factors decide the magnitude (distance) of spatial shift?

- Strength of magnetic field
- Bandwidth of the slice-selective pulses
- Strength of the magnetic field gradient
- Data-sampling bandwidth
- Voxel dimensions
- The chemical shift itself

CSMA – Frequency Encoding

- During data acquisition the MR signal is recorded in the presence of a frequency-encoding gradient. The frequency-encoding gradient G_x (also called the readout gradient) forces water proton spins located at a position X_w along the frequency-encoding axis to precess with a frequency ν_w , which is linearly dependent on position:

$$\nu_w = \gamma G_x X_w$$

CSMA – Frequency Encoding

- The precessional frequency of fat spins ν_F originating at an identical position will differ by the chemical shift between the water and fat resonance

$$u_F = gG_x X_w - du$$

- With Fourier transformation, fat will be mapped into an apparent position

$$X_F = (u_w - du) / gG_x$$

- The resulting mismapping from the original spatial position of the fat spins will be

$$\Delta x = X_w - X_F = du / gG_x$$

CSMA – Frequency Encoding

- The field of view in the frequency direction, the bandwidth of data acquisition, and the readout gradient are related through the formula

$$BW = gFOV \cdot G_x$$

- FOV can be expressed as a product to the number of pixels in the frequency direction and the pixel length

$$FOV = N_x dx$$

- As such, the formula for a CSMA measured in pixels can be written as follows:

$$\Delta x / dx = (du / BW) N_x$$

CSMA – Frequency Encoding

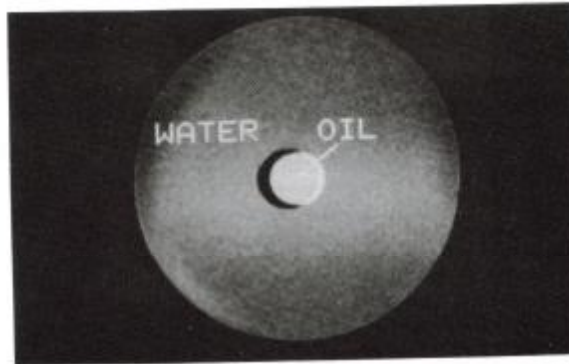


Figure 16-11. CSMA in the frequency-encoding direction. An axial image of a vial containing oil immersed in the larger tank with water, acquired using a whole-body MR scanner operating at 1.5 T. The image of oil is shifted relative to its true position in the water tank. This results in the characteristic dark band/bright band pattern, as illustrated schematically in Figure 16-10.

CSMA – Slice Selection

- The 2D spin-echo MR imaging process is initiated with a **limited bandwidth**, radiofrequency excitation pulse executed in the presence of a slice-selection gradient, G_z . The spatial location of the slice in the z direction will be different for fat and water such that:

$$\Delta z = du / gG_z$$

CSMA – Slice Selection

- The slice thickness dz depends on the bandwidth of the excitation pulse (bw) and strength of the slice-selection gradient G_z , as follows:

$$dz = BW / gG_z$$

- Therefore, CSMA in the slice-selection direction, measured in units of slice thickness, can be written as:

$$\Delta z / dz = du / BW$$

CSMA – Phase encoding

- No observable CSMA occurs in the phase encoding direction in spin-echo imaging. Why?

In each step of spin-echo imaging, the phase acquired by fatty protons differs from water protons in the same location by the effect of chemical shift. However, the resulting extra phase of fat spins relative to water is **not cumulative**; it is the **same for each phase encoding step**, yielding **the same phase encoding differences for each location along the y axis**.

CSMA – Phase encoding

Table 16-2. Phase acquired by water and fat protons at position y during phase encoding by spin-warp method

Phase-encoding step	Water magnetization phase	Fat magnetization phase
N	$2\pi N\gamma G_y y T$	$2\pi N\gamma G_y y T - 2\pi\delta\nu T$
$N + 1$	$2\pi (N + 1)\gamma G_y y T$	$2\pi(N + 1)\gamma G_y y T - 2\pi\delta\nu T$
Phase difference	$2\pi\gamma G_y y T$	$2\pi\gamma G_y y T$

H₂O/Water Signal Separation

- Frequency-selective pulse
- Tissue nulling with inversion recovery
- Dixon method

Frequency-selective pulse

- Selective excitation of the fat magnetization before the imaging sequences to get H₂O image
- Selective excitation of the water magnetization before the imaging sequences to get fat image

Selective excitation of the fat

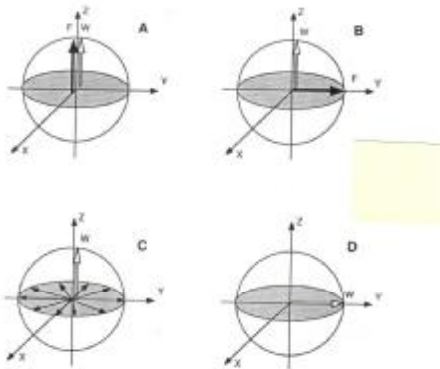


Figure 16-29. Frequency-selective excitation. A, Fat and water magnetizations are initially polarized along the direction of the external magnetic field (Z). B, The selected spectral component (in this case fat) is rotated into the transverse plane by an RF pulse in the absence of a gradient. C, The magnetization is then dephased by a spoiler gradient such that the transverse magnetization of fat averages to zero. D, A slice-selective pulse next rotates the other component (in this case water) into the transverse plane for imaging.

Selective excitation of the fat

- A selective-excitation pulse to rotate the fat magnetization 90 degrees into the transverse xy plane as implemented in the **chemical shift selective sequence (CHESS)**
- Immediate application of a **spoiling gradient** disperses these transverse magnetization so that the **net transverse magnetization is averaged to zero**
- The unexcited **water signal magnetization remains in the z axis** and then using spin-echo, gradient echo etc.

Frequency-selective pulse

- Limitation
Rely on the well-defined frequency separation of water and fat resonance over the FOV
Any inhomogeneity of the magnetic field broadens the resonance line width

Inhomogeneity effects in frequency-selective methods

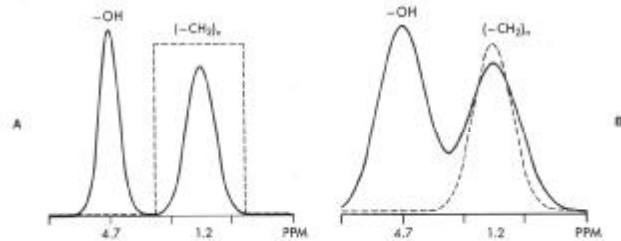


Figure 16-32. Inhomogeneity effects in frequency-selective methods. The resonance lines of water (left) and fat (right) protons are well separated in highly homogeneous magnetic fields. **A.** Application of a frequency-selective pulse with an idealized frequency profile (dashed line) would tip fat protons into the transverse plane without affecting the water protons. **B.** In a typical whole-body magnet, with increasing field inhomogeneities the resonance lines become broadened and less well separated. Application of the frequency-selective pulse with a more realistic profile (dashed line) will leave some of the fat protons unaffected, resulting in a less-than-total fat proton excitation and some unwanted excitation of water protons.

Tissue Nulling with Inversion Recovery

- Eliminating signal from fat is to take advantage of the **differences between T1 tissue relaxation time** by using an inversion recovery sequence

Tissue Nulling with Inversion Recovery

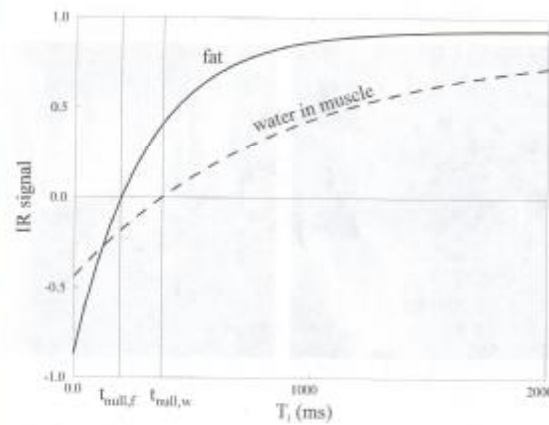


Fig. 17.6: Inversion recovery signal behavior and the choice of the recovery period to null a specific tissue. If data can be collected at the zero crossing (null point) of fat $T_1 = t_{null,f}$ or water $T_1 = t_{null,w}$ that particular tissue can be suppressed from the image. In this figure, fat and muscle (with essentially no fat component) signals are plotted for an IR sequence using a $1.8 T_R$. From Eq. 17.8, the null point for tissues in the finite T_R case is given by $T_{1,null} = T_1 \ln \frac{2}{(1 + e^{-T_R/T_1})}$. For T_R much greater than T_1 , $T_{1,null}$ is usually 150 to 170 ms for fat at 1.5 T.

Tissue Nulling with Inversion Recovery and Frequency-selective Pulse



Fig. 17.7: (a) Fat-saturated image obtained using an inversion time (T_I) of 130 ms. (b) Water-saturated image obtained using a T_I of 300 ms. Both IR images were acquired with a T_R of 1 sec. As is seen from the curves plotted in Fig. 17.6, $t_{null,w}$ for water in the muscle is about 300 ms. This is what is observed in (b). In (c) and (d), a frequency-selective saturation pulse was used. (c) Fat-saturated image, and (d) water-saturated image. In (c) it is apparent that the static field is not well locked to the knee (arrow) so some of the fat has not been fully saturated (compare with image 1 and also the phase in Fig. 17.16 in the same region).

Tissue Nulling with Inversion Recovery

- Limitation

Need long T_R to all tissues to return to M_0

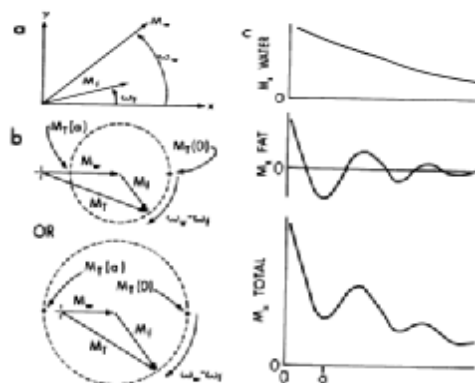
Anyway to overcome it?

Echo Planar Imaging (EPI)

Dixon method

- First introduced in “Dixon WT: Simple proton spectroscopic imaging. Radiology 153: 189, 1984”

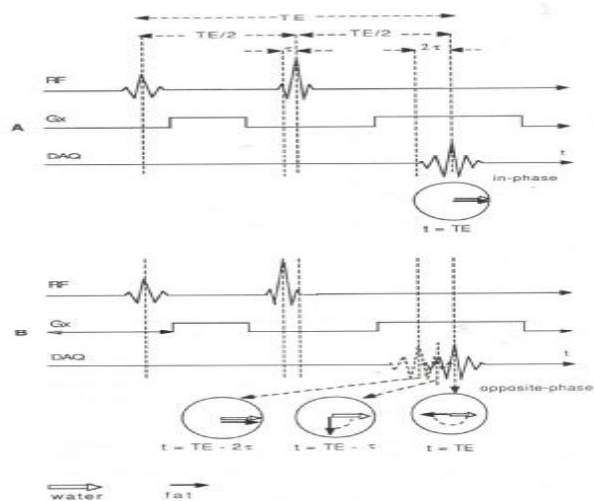
Dixon method



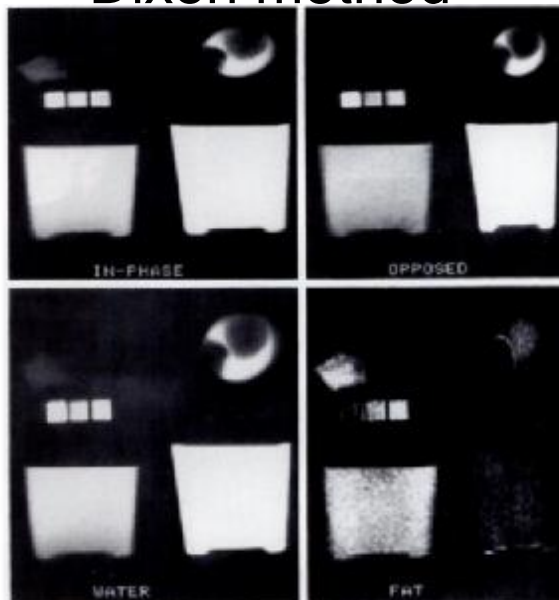
Transverse magnetization following a 90° pulse. The volume element contains both water and fat. M_w = water magnetization; M_f = fat magnetization; ν_w and ν_f = Larmor frequencies of water and fat ($\omega = 2\pi\nu$).

- Laboratory frame.
- Rotating frame, top $|M_w| > |M_f|$, bottom $|M_f| > |M_w|$.
- Typical FID.

Dixon method



Dixon method



Dixon method

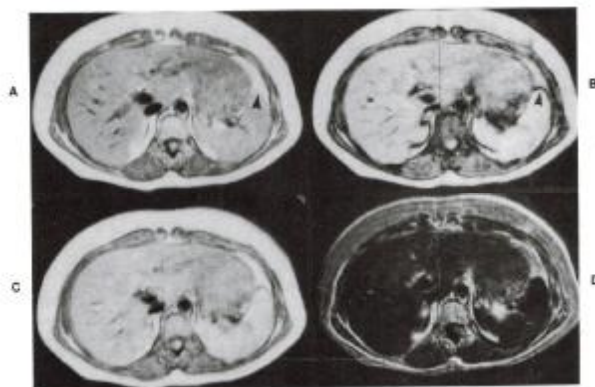


Figure 16-24. Phase-contrast imaging of the liver in a normal volunteer. **A**, Conventional in-phase SE 1500/30 image shows the spleen to have a slightly higher signal intensity than liver. **B**, Opposite-phase SE 1500/30 image again shows the spleen to have a slightly higher signal intensity than the normal, nonfatty liver. A dark band of low signal intensity (arrowheads) demarcates interfaces between water-containing viscera and fat-containing adipose tissue. **C**, Calculated "water-only" image is derived by adding images **A** and **B**. This image is similar to the in-phase image (**A**), indicating that all the liver and spleen signal intensities are from water. **D**, Calculated "fat-only" image is derived by subtracting image **B** from image **A**. The absence of signal from the spleen and liver indicates that neither tissue contains MR-observable fat. The mottled appearance of subcutaneous fat results from the magnitude reconstruction, as explained in Figure 16-23 (Courtesy: D Stark.)

Dixon method Disadvantages

- Necessity for image postprocessing required after acquisition of two independently acquired scans
- What's the other?
Patient motion between each acquisition causes the image artifacts

Reference

- David D.S. et al: Magnetic resonance imaging (Second Edition), 1992
- Haacke E.M. et al: Magnetic resonance imaging physical principle and sequence Design
- Dixon WT: Simple proton spectroscopic imaging. Radiology 153: 189, 1984
- Haase A: H NMR chemical shift selective (CHESS) imaging. Phys. Med. Biol., 1985, Vol. 30, No. 4, 341-344.

HW 1

- Assume that a voxel centered at x_0 with width Δx contains both water and fat uniformly distributed throughout the voxel
- a) How large must the read gradient G_R be so that 80% of the fat lies within the same voxel as the water when $\Delta x = 1\text{mm}$? Assume that all the fat sits at one frequency with $\Delta f = 3.35\text{ppm}$ and $B_0 = 1.0\text{T}$.
- b) In what direction along x is fat shifted

Hw 2

- Derive the equation of the correct timing offset τ of the 180 degree pulse to create an opposite-phase image